Applied Surface Science 257 (2010) 37–41

Contents lists available at ScienceDirect

Applied Surface Science

journal homepage: www.elsevier.com/locate/apsusc

Nanoscratch study of $Zn_{1-x}Mn_xO$ heteroepitaxial layers

Yu-Ming Chang[a], Zue-Chin Chang[b], Derming Lian[b], Chu-Shou Yang[c], Wei-Hung Yau[b], Chien-Huang Tsai[d,*], Wen-Fa Wu[e], Chang-Pin Chou[a]

[a] Institute and Department of Mechanical Engineering, National Chiao Tung University, Hsinchu 300, Taiwan, ROC
[b] Department of Mechanical Engineering, Chin-Yi University of Technology, Taichung 400, Taiwan, ROC
[c] Graduate Institute of Electro-Optical Engineering, Tatung University, Taipei 10452, Taiwan, ROC
[d] Department of Automation Engineering, Nan Kai University of Technology, 568 Chung-Cheng RD, Nantou 54243, Taiwan, ROC
[e] National Nano Device Laboratories, Hsinchu 300, Taiwan, ROC

ARTICLE INFO

Article history:
Received 27 October 2009
Received in revised form 7 April 2010
Accepted 10 June 2010
Available online 17 June 2010

Keywords:
Molecular beam epitaxy
Scanning electron microscopy
Transmission electron microscopy

ABSTRACT

We investigated the nanotribological properties of $Zn_{1-x}Mn_xO$ epilayers ($0 \le x \le 0.16$) grown by molecular beam epitaxy (MBE) on sapphire substrates. The surface roughness and friction coefficient (μ) were analyzed by means of atomic force microscopy (AFM) and hysitron triboscope nanoindenter techniques.

The nanoscratch system gave the μ value of the films ranging from 0.17 to 0.07 and the penetration depth value ranging 294–200 nm when the Mn content was increased from $x = 0$ to 0.16. The results strongly indicate that the scratch wear depth under constant load shows that higher Mn content leads to $Zn_{1-x}Mn_xO$ epilayers with higher shear resistance, which enhances the Mn–O bond. These findings reveal that the role of Mn content on the growth of $Zn_{1-x}Mn_xO$ epilayers can be identified by their nanotribological behavior.

1. Introduction

ZnO, one of the II–VI compound semiconductors, has a hexagonal wurtzite crystal structure ($a = 3.249$ Å, $c = 5.2057$ Å). It has a high coupling factor as well as simple composition as a piezoelectric material [1]. In recent years, diluted magnetic semiconductors (DMSs) have been found to play an important role in interdisciplinary material science, especially in magneto- and spin-electronics [2]. Mn-based II–VI alloys have found increasing commercial applications due to their properties such as hardness (H), Young's modulus, corrosion resistance, magnetic properties, and electrical properties [3–9].

These structures are expected to be more reliable because their band gaps can be easily controlled by choosing the Mn content. However, the mechanical damage usually suppresses the processing yield as well as application reliability of microelectronic devices. The traditional approach involves improving the properties such as nanohardness, Young's modulus, thermal drift and corrosion resistance by increasing the coating thickness, which is no longer valid. These properties must be enhanced through the basic improvement of the intrinsic properties of the thin film through the composition or the extrinsic properties including structure, grain size, morphology, etc. H and residual stress are important parameters for tribological coatings [10,11]. Measurements can evaluate material properties such as the interface delamination, bonding, cracking, etc. [12–14]. In early works, the structures of Mn- [15] and Be-based [16,17] II–VI alloys have found increasing commercial applications. The improvements in their mechanical properties have also increased their processing quality [18–20]. However, evidence of the effect of Mn content on the crystal properties of ZnO has not been satisfying until now. In this work, the nanoscratch system was employed to investigate the nanotribological behavior of $Zn_{1-x}Mn_xO$ epilayers. Stronger interface adhesion and lower coefficients of friction with increased Mn content were found.

2. Experimental details

The $Zn_{1-x}Mn_xO$ epilayers were grown on a sapphire substrate with a Veeco Applied EPI 620 Molecular Beam Epitaxy (MBE) system. The Veeco Applied EPI 40cc low-temperature cells were employed to evaporate the elemental solid sources (Zn and Mn). The substrate temperature was 650 °C; the thickness of the $Zn_{1-x}Mn_xO$ layer for each sample was about 800–900 nm. Energy dispersive X-ray spectroscopy (EDS) was used to determine the Mn content ($x = 0$, 0.09, and 0.16). Furthermore, in order to identify the nanotribological properties of samples, atomic force microscopy (AFM, Digital Instruments Nanoscope III) together with a nanoindentation measurement system (Hysitron Inc.) was used to perform the nanoscratch tests, in which a constant scan speed of 2 $\mu m\,s^{-1}$ was used. For samples of $Zn_{1-x}Mn_xO$ epilayers/sapphire systems,

* Corresponding author.
E-mail address: chtsai12@gmail.com (C.-H. Tsai).

0169-4332/$ – see front matter © 2010 Elsevier B.V. All rights reserved.
doi:10.1016/j.apsusc.2010.06.027

various constant forces (1000, 2000, and 3000 μN) at different Mn contents (x = 0, 0.09, and 0.16) were used. The maximum load was then maintained during the 10-μm-long scan. Surface profiles before and after scratching were obtained by scanning the tip at a 0.02-mN normal load, a load sufficiently small that it produced no measurable displacement. After scratching, the wear tracks were imaged by AFM.

3. Results and discussion

The three-dimensional AFM images of $Zn_{1-x}Mn_xO$ epilayers deposited with different Mn contents (x = 0, 0.09, and 0.16) are shown in Fig. 1. Clearly, the surface morphologies of the films became smooth, and grains grew and were distributed uniformly with higher Mn content. It is suggested that the sapphire substrate surface does not have a specific epitaxial orientation to follow, which results in randomly oriented nuclei. The R_{ms} (root mean square) surface roughness of $Zn_{1-x}Mn_xO$ epilayers slightly decreased from 6.2 and 5.3 nm to 5.1 nm with increasing Mn content.

Fig. 2 shows three typical AFM profiles, where the lateral forces were a normal constant load of 1000 μN for all of the samples. In addition, it is interesting to point out that the features of the nanoscratch zone in the vicinity of the interface may not be just accidental artifacts resulting from sample preparation. In the cross-section height profile, one can easily see that the nanoscratch depths, corresponding to ZnO and ZnMnO, do not show a linear relationship with the applied normal load. The profile of the ZnO sample is softer than that of ZnMnO. The shape and height of the pile up (or sink-in) depend on the ratio E (elastic modulus)/Y (yield strength) of the sample and the strain-hardening exponent. In general, pile up is generated when most of the plastic deformation occurs near the diamond tip; it occurs markedly for non-strain-hardening materials having large values of E/Y. In addition, the existence of a compressive residual stress of a moderate magnitude is beneficial to the film, because it can suppress crack initiation. The transitions were determined from the nanoscratch traces and pile up. Bulge edge scenarios can be observed between the groove and film, and therefore the material was crushed as a result of plastic deformation. These conditions are evidence that the significantly reduces the average nanoscratch depth from x = 0 to 0.09 [Fig. 2(a) and (b)], for example. This reduction may be due to the Mn stoichiometry in the ZnO microstructure, which results in uneven local deformation recovery. Furthermore, we observe the nanoscratch deformation for x = 0.16 [Fig. 2(c)] within the shallow profile of the nanoscratch traces, which may be because the Mn–O bond is stronger than the Zn–O bond. It is also can be observed that the depth profile are 294, 215, and 200 nm (Mn stoichiometry x = 0, 0.09, and 0.16) from the insert image of Fig. 2, which implies that the $Zn_{1-x}Mn_xO$ epilayers at higher Mn contents have a stronger adhesion at the interface.

Fig. 3 shows three typical profiles of the coefficient of friction (μ) vs. scratch duration, obtained as the ratio of the in situ measured tangential force to the applied normal load. The scan profile can be divided into three steps according to time: (1) the pre-approach time (0–12 s), in which the tip does not penetrate the film or the profile; and (2) the residual depth region time (12–42 s), in which the superficial profile is essentially controlled by plasticity and H, showing the recovery behavior and the elasto-plastic deformation of the film. The fluctuation profile from the nanoscratch tests does not depend exclusively on plasticity and H. It is related to the adhesive strength between the film and the substrate [21]. Finally, the third stage is (3) the post-approach time (over 42 s), in which the tip leaves the film. Afterward, the μ profile oscillates more or less regularly due to the ZnO bond, or rather the cohesive failure from

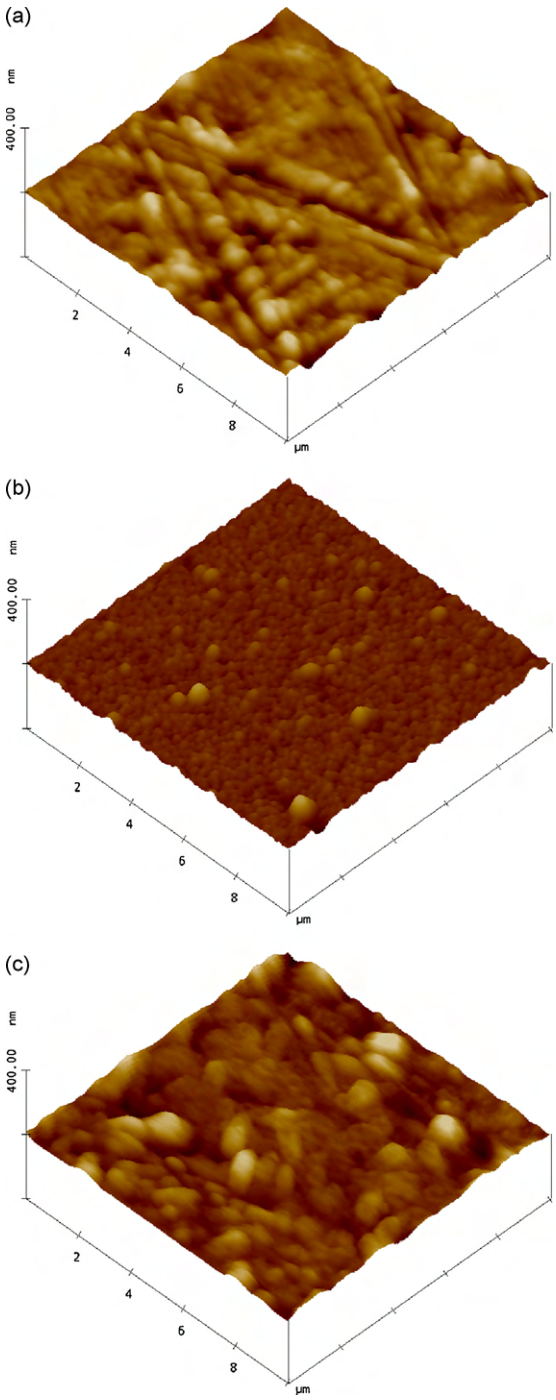

Fig. 1. AFM images of surfaces of ZnO thin films deposited with Mn stoichiometry x = (a) 0, (b) 0.09, and (c) 0.16.

the period of transition between the Zn–O bond and weaker Mn–O bond [Fig. 3(a) and (b)]. Accordingly, the frictional force reflects a sliding mechanism in operation at a Mn content of x = 0.16, and a stronger adhesion of the film was observed as the slight fluctuation of the μ profile under the nanoscratch tests [Fig. 3(c)]. Such strong adhesion reflects the interlinks and rearrangements within higher Mn-content interfaces involving not only the stronger MnO bond but also the surface activation, resulting in the lower value of the depth profile and the μ value signals. From the nanotribological viewpoint, the curvature and/or distribution of the μ value signals the onset of adhesive failure such as cracking or delamination [16,21,22], resulting from the interaction between the sliding

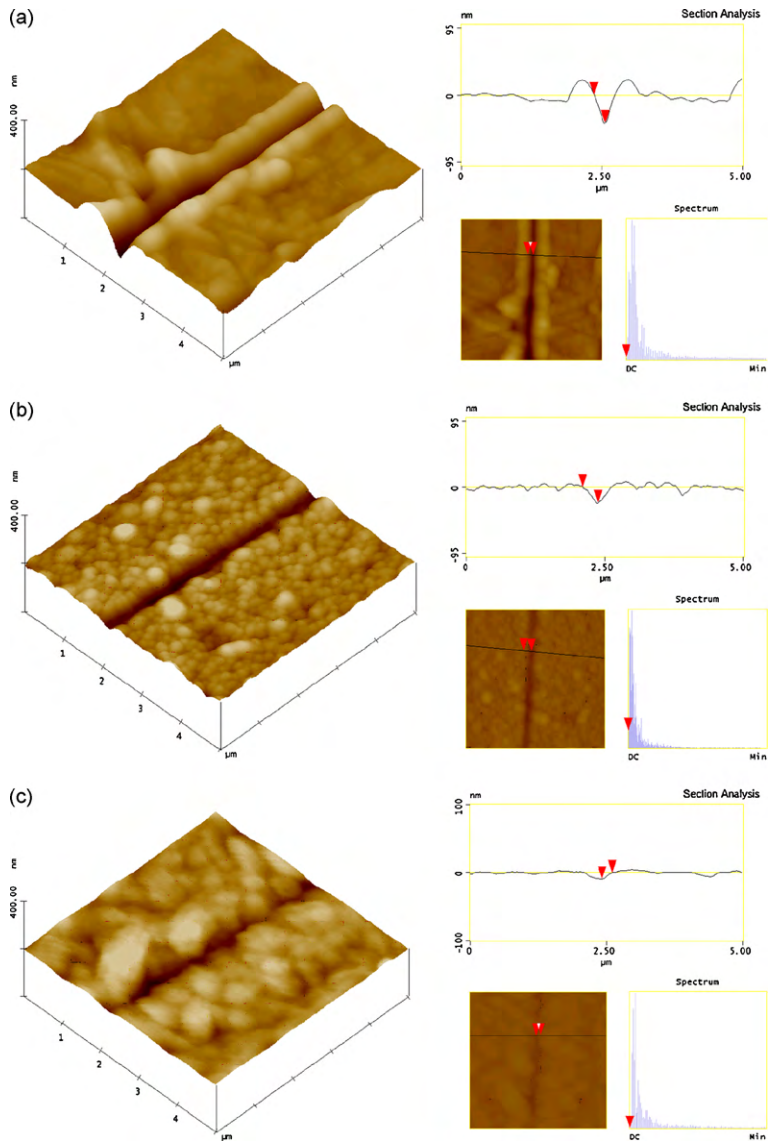

Fig. 2. AFM together with a nanoindentation measurement system was used to perform the nanoscratch tests; the images of the depth profiles are 294, 215, and 200 nm, respectively. (Mn stoichiometry x = (a) 0, (b) 0.09, and (c) 0.16.)

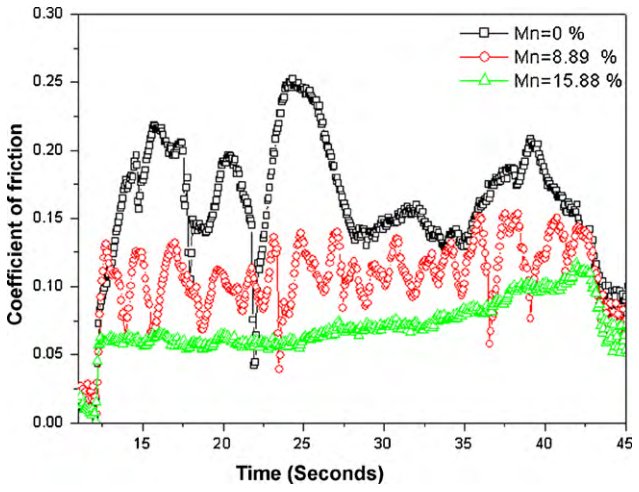

Fig. 3. Three typical profiles of the coefficient of friction (μ) vs. scratch duration at different Mn contents of the $Zn_{1-x}Mn_xO$ epilayers/sapphire system. (Mn stoichiometry x = (a) 0, (b) 0.09, and (c) 0.16.)

stylus and the debris formed on the nanoscratch track. As Sreekantha Reddy et al. reported [15], the resistivity also showed a definite decrease with increasing Mn concentration in the $Zn_{1-x}Mn_xS$ alloy. Grillo et al. also reported [16] that the mechanical properties of ZnSe are significantly improved by alloying with BeSe. They suggested an abrupt change in the mechanical properties of ZnBeTe at the Be-based bond percolation threshold [17]. It is known that several factors could affect the H of the film, such as the packing factor, stoichiometry, residual stress, preferred orientation and grain size. In our results, the Mn content not only enhanced the ZnO bond but also increased scratching resistance comparatively. That is to say, the volume of the material removed can be employed to evaluate the role of the Mn content by using the nanoscratch technique. The results support an explanation in terms of the nanotribological behavior of the $Zn_{1-x}Mn_xO$ epilayers, such as the result shown in Fig. 3. A similar reference reported the details of film quality and the relative characterizations of $Zn_{1-x}Mn_xO$ [16].

Fig. 4 also illustrates AFM images with a nanoindentation measurement system made at various normal loads, from 1000 to 3000 μN, on the three different samples, together with the corresponding cross-sectional height profiles. The observation of a

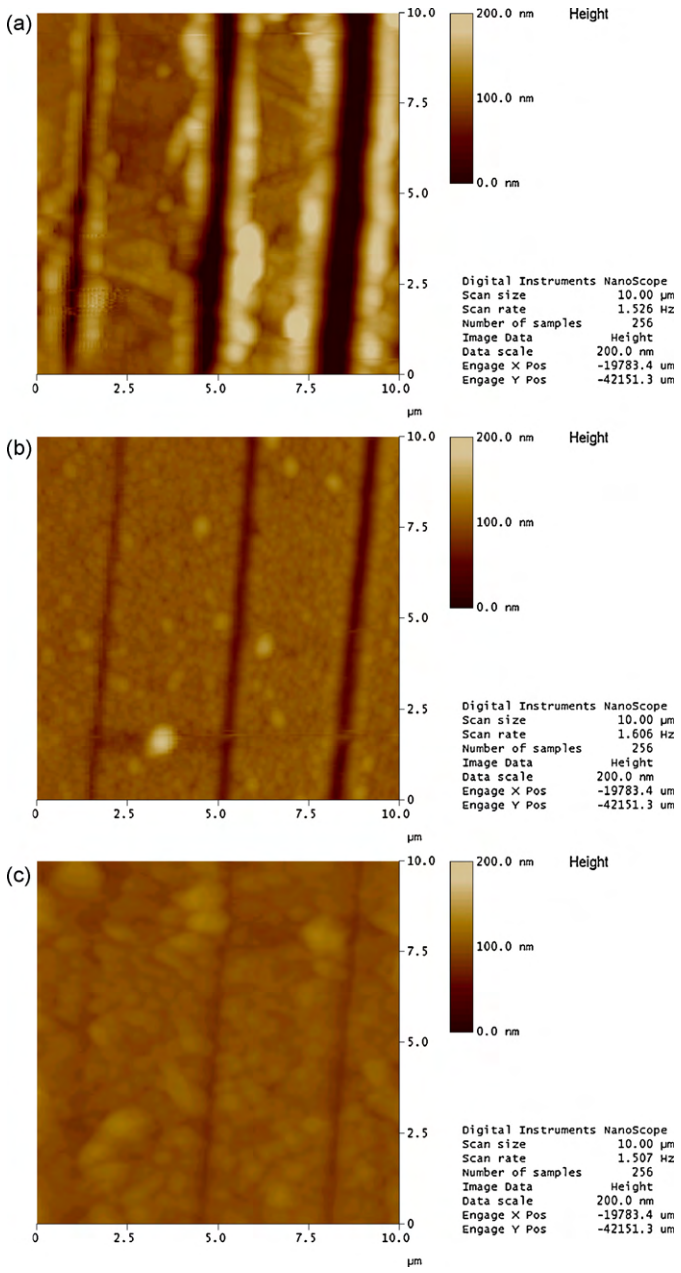

Fig. 4. AFM together with a nanoindentation measurement system was used to perform the nanoscratch tests; the images of the depth profiles of the nanoscratch traces were provided with various constant forces (1000, 2000, and 3000 μN) at different Mn contents of the $Zn_{1-x}Mn_xO$ epilayers/sapphire system. Mn stoichiometry x = (a) 0, (b) 0.09, and (c) 0.16.

compressive residual stress of moderate magnitude is beneficial to the film because it can suppress crack initiation. However, these images are partially altered in terms of the orientation of the tip and scratch direction. This phenomenon is similar to a previous report, and the stick–slip effect usually occurs in the crystal orientation of the semiconductor materials [23]. As is generally known, stick–slip is the intermittent relative motion of two sliding surfaces against each other. On dry metallic surfaces, the frictional force is not constant during sliding but has a sawtooth wave form, and the sliding motion proceeds by jerks instead of a smooth path [24]. Li et al. reported that a "joint" was formed during stick, and during slip a uniform "stem" is found in the morphology of the scratch with the force curve [24]. The stick–slip motion is a typical friction-induced vibration observed at small sliding speeds. During scratching, it is suggested that the sample or the indenter is driven through elastic members, and the stick–slip phenomenon may be observed [24–27]. From prior works [28,29], the low friction coefficient of nanocrystalline ZnO is owing to the presence of a mosaic of low-angle grains within the nano-columns. It is suggested that the both films and substrates often have different thermal properties, resulting in strain when the films are deposited under elevated temperatures. Grain growth and strain energy are processed at the film surface and at the film–substrate interface. Strain energy can often be a dominant factor, which is usually plays a critical role at different film (substrate orientations). In general, the mechanical properties of $Zn_{1-x}Mn_xO$ films can also influence the dominant crystal texture at higher Mn contents. In closing, three scratches were made on the same specimen for various vertical loads at the same driving speed of 2 $\mu m\,s^{-1}$. Stick–slip motion was found, whereas the period and amplitude of stick–slip, which were averaged over each test, increased with the normal load. The profile of the pure ZnO sample shows serious wear of the components (Fig. 2) and more unwanted self-excited oscillations (Fig. 3) and positioning errors (Fig. 4) than the Mn-containing sample. Therefore, $Zn_{1-x}Mn_xO$ epilayers show relatively small oscillations with a Mn content of $x = 0.09$ and stable oscillations with a Mn content of $x = 0.16$. The pure ZnO sample may stick together until the elastic forces become sufficient to jerk them loose, and sliding occurs until the sample become stuck again and the elastic forces decrease to certain limits.

4. Conclusion

The contact-induced structural deformation behaviors of MBE-derived $Zn_{1-x}Mn_xO$ epilayers are reported here. The nanotribological behavior was determined from nanoscratch traces, pile up, and bulge edge on the groove in the film due to the material being crushed as a result of plastic deformation. Accordingly, the frictional force reflects a sliding mechanism that operates at a Mn content of $x = 0.16$, and stronger adhesion of the film was observed with slight fluctuation of the μ profile during the nanoscratch tests. The frictional force of the ZnO sample was not constant during sliding but had a sawtooth wave form, and the sliding motion proceeded by jerks instead of a smooth path due to the stick–slip phenomenon. It is suggested that the Mn–O bond is stronger than the Zn–O bond from nanotribological observation.

Acknowledgment

This research was supported by the National Science Council in Taiwan under contract NSC 98-2216-E-009-069 and by National Nano Device Laboratories in Taiwan under Contract NDL98-C03SP-128 and NDL98-C03SP-127. The author would like to thank professor Chu-Shou Yang for help with the samples preparation and kindly discussion.

References

[1] K.H. Yoon, J.W. Choi, D.H. Lee, Thin Solid Films 302 (1997) 116.
[2] Ryan P. Davies, C.R. Abernathy, S.J. Pearton, D.P. Norton, M.P. Ivill, F. Ren, Chem. Eng. Commun. 196 (2009) 1030.
[3] A. Che Mofor, A. El-Shaer, A. Bakin, H.H. Wehmann, H. Ahlers, U. Siegner, S. Sievers, M. Albrecht, W. Schoch, N. Izyumskaya, V. Avrutin, J. Stoemenos, A. Waag, Superlattices Microstruct. 39 (2006) 381.
[4] V. Avrutin, N. Izyumskaya, Ü. Özgür, A. El-Shaer, H. Lee, W. Schoch, F. Reuss, V.G. Beshenkov, A.N. Pustovit, A. CheMofor, A. Bakin, H. Morkoç, A. Waag, Superlattices Microstruct. 39 (2006) 291.
[5] H.J. Lin, D.Y. Lin, J.Z. Hong, C.S. Yang, C.M. Lin, C.F. Lin, Phys. Stat. Solid. (C) 6 (2009) 1468.
[6] S.W. Jung, S.J. An, G.C. Yia, C.U. Jung, S.I. Lee, S. Cho, Appl. Phys. Lett. 80 (2002) 4561.
[7] Ü. Özgür, Ya.I. Alivov, C. Liu, A. Teke, M.A. Reshchikov, S. Doğan, V. Avrutin, S.J. Cho, H. Morkoç, J. Appl. Phys. 98 (2005) 041301–041311.

[8] M. Godlewski, J.P. Bergman, B. Monemar, E. Kurtz, D. Hommel, Appl. Phys. Lett. 69 (1996) 2843.
[9] W. Meredith, G. Horsburgh, G.D. Brownlie, K.A. Prior, B.C. Cavenett, W. Rothwell, A.J. Dann, J. Cryst. Growth 159 (1996) 103.
[10] M.A. Haase, J. Qiu, J.M. Depuydt, H. Cheng, Appl. Phys. Lett. 59 (1991) 1272.
[11] T. Dharma Raju, K. Nakasa, M. Kato, Acta Mater. 51 (2003) 457.
[12] S.J. Bull, J. Phys. D 38 (2005) R393.
[13] G.M. Pharr, A. Bolshakov, J. Mater. Res. 17 (2002) 2660.
[14] W.C. Oliver, G.M. Pharr, J. Mater. Res. 19 (2004) 3.
[15] D. Sreekantha Reddy, B. Kang, S.C. Yu, Y. Dwarakanadha Reddy, S.K. Sharma, K.R. Gunasekhar, K.N. Rao, P. Sreedhara Reddy, Curr. Appl. Phys. 9 (2009) 431.
[16] S.E. Grillo, H. Glénat, T. Tite, O. Pages, O. Maksimov, M.C. Tamargo, Appl. Phys. Lett. 93 (2008) 08190.
[17] S.E. Grillo, M. Ducarroir, M. Nadal, E. Tournié, J.P. Faurie, J. Phys. D: Appl. Phys. 35 (2002) 3015.
[18] S.Y. Chang, T.Q. Chang, Y.S. Lee, J. Electrochem. Soc. 10 (2005) C657.
[19] P.A. Steinmann, H.E. Hintermann, J. Vac. Sci. Technol. A7 (1989) 2267.
[20] X. Li, F. Huang, M. Curry, S.C. Street, M.L. Weaver, Tribol. Lett. 19 (2005) 273.
[21] J.M. Sánchez, S. El-Mansy, B. Sun, T. Scherban, N. Fang, D. Pantuso, W. Ford, M.R. Elizalde, J.M. Martínez-Esnaola, A. Martín-Meizoso, J. Gil-Sevillano, M. Fuentes, J. Maiz, Acta Mater. 47 (1999) 4405.
[22] R. Saha, William D. Nix, Acta Mater. 50 (2002) 23.
[23] A. Richter, B. Wolf, J. Belbruno, Solid State Phenom. 95–96 (2004) 519.
[24] K. Li, B. Yuhong Ni, J.C.M. Li, J. Mater. Res. 11 (1996) 1574.
[25] F.P. Bowden, L. Leben, Proc. R. Soc. Lond. A 169 (1939) 371.
[26] C.M. Mate, G.M. McClelland, R. Erlandsson, S. Chiang, Phys. Rev. Lett. 59 (1987) 1942.
[27] K. Khurana, Phys. Today 41 (5) (1988) 17.
[28] S.V. Prasad, S.D. Walck, J.S. Zabinski, Thin Solid Films 360 (2000) 107.
[29] Y.R. Jeng, H.C. Wen, P.C. Tsai, Diamond Relat. Mater. 18 (2009) 528.